

8th U. S. National Combustion Meeting
Organized by the Western States Section of the Combustion Institute
and hosted by the University of Utah
May 19-22, 2013

Solid Propellant Combustion Enhancement Using Fluorocarbon Inclusion Modified Aluminum

Travis R. Sippel, Steven F. Son, Lori J. Groven

*School of Mechanical Engineering, Purdue University
500 Allison Road
Chaffee Hall
West Lafayette, IN 47906 USA*

Abstract

The use of aluminum in solid propellants improves performance, but theoretical performance is not reached primarily because of two-phase flow losses. These losses could be reduced if particles ignited sooner rather than agglomerating before ignition, or if particles were dispersed when they burned. In order to modify the ignition and combustion of aluminum particles, the use of mechanically activated (MA) composite particles (Al/PTFE 70/30 wt.%) as a replacement for spherical, micron-sized aluminum in a composite solid propellant and their effects on burning rate, pressure dependence, and aluminum ignition, combustion, and agglomeration is considered here. Use of these modified Al particles, instead of micron-sized Al, results in an increase in pressure dependence (from 0.36 to 0.58) and a corresponding 55% increase in burning rate at a pressure of 15 MPa. Atmospheric observation of the burning surface suggests this increased dependence on pressure is a result of dramatically reduced burning particle size and the smaller particles sizes leads to kinetically controlled combustion. Unlike spherical aluminum, Al/PTFE composite particles promptly ignite at the propellant surface and fragment into smaller burning particles that are consumed closer to the surface. To capture these particles from burning propellant, a unique, solvent-free quench technique is used to minimize contamination and sampling error. Analysis of quenched combustion products collected on a substrate at pressure (2.1 to 13.8 MPa) just above the burning surface indicates these smaller burning particles result in a decrease in average agglomerate size from 76 μm to 25 μm (a 96% decrease in agglomerate volume), from the baseline and modified Al propellants, respectively. Analysis of these products from the modified Al propellant using scanning electron microscopy and energy dispersive spectroscopy indicate the presence of a fine ($< 1 \mu\text{m}$) particle fraction comprised of aluminum oxide and aluminum fluoride as well as a coarse fraction of aluminum oxide agglomerates, in contrast to the baseline propellant that shows significant unburned Al at the same collection height. In propellant applications, these effects are expected to translate to a decrease in two-phase flow loss and reduced slag accumulation, which could result in improved performance.

1. Introduction

Aluminum is commonly used as an ingredient in propellants, explosives, and pyrotechnics, as it has a high gravimetric and volumetric combustion enthalpy that results in significant performance increases. For example, the use of aluminum in composite solid propellants can improve specific impulse performance by as much as 15% [1]. This performance increase follows from an increase in flame temperature and a decrease in gaseous product molecular weight (a shift from CO_2 and H_2O to CO and H_2 in propellant exhaust products). However, there are several drawbacks to the use of aluminum. First, micron-scale aluminum has a high ignition temperature ($\sim 2000 \text{ }^\circ\text{C}$). Second, use of aluminum in a solid propellant results in coalescence of liquid aluminum (agglomeration) at the

burning surface of the propellant. As these large agglomerates flow through a motor, they slow the velocity of surrounding gaseous products and fail to liberate their thermal energy to the flow. These effects are termed two-phase flow losses and can reduce performance by as much as 10% [1] and prevent theoretical performance levels from being achieved.

In efforts to overcome these drawbacks, the use of more finely divided nanoscale aluminum (nAl) produces smaller agglomerates [2] and can potentially result in kinetically rather than diffusionally limited metal combustion [3]. Nanoscale particles can have a number of desirable effects such as shorter aluminum burning time (which translates to additional radiation heat transfer to the propellant surface) as well as a reduction in particle ignition temperature and an increase in burning rate pressure dependence. However, use of nAl (as well as every other enhancement technique tried to date) results in product particle sizes that are larger than initial particle sizes. Additionally, the high specific surface area of nAl ($\sim 10\text{-}50\text{ m}^2/\text{g}$) decreases propellant specific impulse (through the presence of additional aluminum oxide in the original material), and can result in high uncured propellant viscosity [4] and poor mechanical strength [5]; which together can decrease propellant density, produce erratic combustion, or even motor failure. As a consequence, nanoscale aluminum is not used in typical solid propellants.

Alternately, improved reactivity and decreased agglomeration could be achieved through the use of overall micrometer-scale aluminum that contains nanoscale inclusions of a separate material to potentially realize the benefits of nanoscale particles without the disadvantages. There are examples in the literature of this approach. Low levels (10 at.%) of nickel, iron, or zinc inclusion within aluminum particles [6] as well as inclusion of iodine, paraffin, or low density polyethylene [7, 8] have resulted in decreased ignition temperature and reduced oxidation onset. However, these inclusion materials either result in formation of additional condensed phase products or are not reactive with aluminum. In order to obtain better aluminum ignition enhancement and also reduce two-phase flow losses, it is desirable to select an inclusion material that will both react with aluminum and also form fewer condensed phase products. Disparate thermal expansion and gas production within the particle could lead to particle fragmentation also, yielding much smaller product particle sizes and lower two-phase flow losses. The addition of fluorocarbons could possibly meet these requirements.

In recent work we have shown that inclusion of low levels of polytetrafluoroethylene (PTFE) in aluminum via mechanical activation results in nanofeatures within micrometer-scale particles that have moderate surface areas, high combustion enthalpy (20.2 kJ/g), and have drastically enhanced reactivity [9]. Fluorocarbon inclusions, such as PTFE, are of particular interest for two reasons. First, the gravimetric (9.7 kJ/g) and volumetric (20.5 kJ/cm³) reaction enthalpy of Al/PTFE is very high [9]. Second, fluorination of aluminum results in less condensed phase products (and potentially lower two-phase flow loss) since AlF₃ sublimates at $\sim 1000\text{ }^\circ\text{C}$.

The objective of this work is to determine the agglomeration, burning rate, and metal particle ignition effects of using inclusion-modified, fuel-rich Al/PTFE (70/30 wt%) composite particles as a substitute for micron-sized aluminum in an AP composite propellant.

2. Methods

In this work, fuel-rich mixtures of 70 wt.% Al (35 μm , Valimet H30) and 30 wt.% PTFE (35 μm , Sigma-Aldrich 468096) were mechanically activated in 10 g batches inside 60 mL high density polyethylene containers (McMaster-Carr 42905T23) using a charge ratio of 12 (73 wt.% 0.95 cm (McMaster-Carr 9529K19), 27 wt.% 0.476 cm (McMaster-Carr 9529K13) 440C steel media). Containers were filled with argon (99.997%) prior to mechanical activation (50 min MA time) on a SPEX 8000M high energy mill using a duty cycle of 1 min ON, 4 min OFF. During milling, the container was cooled using a fan. All milled materials were handled in an argon-filled glove box and were passivated prior to use. This was done by adding enough hexane to fully cover the particles and then slowly evaporating the hexane in air. A full characterization (particle size, morphology, specific surface area, combustion enthalpy, and reactivity) of similar Al/PTFE MA composite powders is reported in Ref. [10].

Batches of solid propellant were made using either the MA composite particles or comparable spherical aluminum. Prior to use in propellant, the Al/PTFE MA composite powder was sieved between 25 and 75 μm for six hours using a vibratory table (McMaster-Carr 5817K18). The size distributions (shown in Figure 1) of the sieved MA composite powder as well as a similarly sieved fraction of Valimet H30 spherical aluminum powder were verified using a Malvern Mastersizer 2000 with Hydro 2000 μP dispersion unit and isopropyl alcohol dispersant. Propellant consisted of 14 wt.% of a hydroxyl-terminated polybutadiene (HTPB) binder (cured with isophorone diisocyanate), 71 wt.% ammonium perchlorate (AP) (80 wt.% coarse 200 μm and 20 wt.% fine 20 μm , ATK), and 15 wt.% of either the sieved spherical aluminum or the sieved MA composite powder. The propellant was mixed in \sim 200 g batches for 20 min using a LabRam (Resodyn) resonant mixer at 90% intensity. Propellant was deaerated for 15 min at < 3.5 kPa (< 0.5 psia) prior to measuring uncured viscosity and temperature using a Brookfield DVII-HD viscometer. Propellant was then packed into 5.8 mm diameter, \sim 6 cm long cylindrical strand molds and was cured in air at 60 $^{\circ}\text{C}$ for at least seven days. After curing, the density of the propellant is measured using the procedure described in Ref. [11].

Propellant agglomerate products were collected using an inert gas combustion vessel and the device shown in Figure 2. Briefly, a 23 mm tall propellant strand is ignited using an electrically heated, 24-gauge nickel-chromium wire. Once the propellant strand burns to a prescribed height, a 10 mW helium-neon laser beam shines across the surface of the burning propellant and into a photodiode detector on the other side of the combustion vessel. This simultaneously triggers both video recording (actually pre-triggered appropriately) of the combustion event (Phantom Miro eX4, 100 frames/sec) for determining linear burning rate as well as the reversal of the voltage polarity to the DC motor. The motor sweeps a borosilicate quench disc (McMaster-Carr 8477K11) past the surface of the burning propellant at a velocity of \sim 7 m/s (a \sim 8 ms delay) and a height of 2-6 mm above the burning surface. During this process condensed products from propellant combustion are quenched on the surface of the borosilicate disc, which then moves to the other side of the combustion vessel where it is protected from the combustion product flow for the remainder of the experiment. This unique quenching technique varies from the solvent quench approach commonly reported [2, 12], and eliminates contamination of the products with the igniter wire, sampling error due to product washing/filtration, variations in products formed during transient startup/burnout and changes in quench height as the sample burns away from the solvent quench.

The borosilicate quench disc was extracted after the experiment and was analysed directly. Surface images were taken using a FEI Quanta 3D-FEG scanning electron microscope. Agglomerate product size was determined by direct measurement (sample size of 100 agglomerates) and agglomerate product phase and composition were determined using electron dispersive spectroscopy (Oxford INCA Xstream-2 silicon drift detector).

3. Results and Discussion

As a result of the particle morphology of Al/PTFE composite particles, there are distinct differences in propellants made from the composite particles and spherical aluminum. While both powders were sieved to 25- 75 μm , Figure 1 shows that a small portion of the size distribution of the Al/PTFE composite particles is below ~ 20 μm in size and overall the Al/PTFE size distribution is broader than that of spherical aluminum. This is a result of differences in the sieving efficiency and the non-spherical morphology of the modified Al particles. However, the average particle size of Al/PTFE composite particles (42.3 μm) is very near that of the spherical aluminum (43.3 μm). These variations in size distribution and morphology have an effect on propellant properties (Table 1). The non-spherical morphology and slightly smaller particle size distribution of the Al/PTFE composite particles resulted in an increase in viscosity from 4.8×10^6 to 4.7×10^7 cP. However, this increase in viscosity does not affect the final, cured propellant density. Cured propellant containing Al/PTFE composite particles had a high density (1.72 g/cm^3 , 90.6% TMD) that was comparable to the density of the propellant containing spherical aluminum (1.68 g/cm^3 , 87.6% TMD).

Images of propellants burning at 1 atm pressure (Figure 3) show a drastic difference in metal particle ignition and combustion that result from use of Al/PTFE composite particles. In the baseline propellant containing spherical aluminum particles, very little combustion of aluminum was observed at the surface and most metal combustion began only after particles had traveled at least ~ 2 mm from the propellant surface. In the image shown in Figure 3, this results in a darker region near the burning surface of the propellant containing spherical aluminum. In sharp contrast, frequent ignition of composite Al/PTFE particles can be seen on the surface. Video of this combustion process also shows that the velocity of Al/PTFE composite product particles is greater than that of the spherical aluminum (velocities of the particles are closer to that of the gas). As the size distributions of the sieved Al/PTFE and spherical aluminum particles were similar, Al/PTFE particle ignition likely results in production of aluminum fluoride gas at Al/PTFE interfaces throughout the interior of the particles, resulting in fragmentation of the composite particles into smaller, faster burning particles.

The result of Al/PTFE MA particle breakup into smaller particles at the burning surface can be further seen in examination of agglomerate products collected at 6.89 MPa (Figure 4). Products contain both a coarse and a fine, sub-micron (not visible in Figure 4) particle fraction. The coarse fraction from baseline propellant containing spherical aluminum is much larger than that of propellant containing Al/PTFE composite particles. Sizing of these agglomerates directly (Figure 5) indicates they are lognormally distributed and that use of Al/PTFE MA composite particles reduces the average agglomerate diameter by 66% from 76 to 25 μm (a particle volume reduction of 96%). This size reduction is significant, as all previous attempts to decrease agglomerate size has resulted in agglomerates that are still larger than initial particle sizes. This is the first work that the authors are aware of in which agglomerate sizes smaller than initial particle sizes have been obtained. This

decrease in condensed product size indicates that the modified Al particles fragment, due to disparate thermal expansion and interparticle gas production.

Measured linear burning rates (Figure 6) show that addition of Al/PTFE composite particles has a significant effect on both propellant burning rate and sensitivity to gas pressure. At low pressures (~2 MPa), burning rates were nearly the same. However, at high pressure (15 MPa), Al/PTFE particles result in a burning rate that is 55% faster than that of propellant containing spherical aluminum. Overall, this results in an increase in propellant pressure sensitivity from 0.36 to 0.58. Previous work examining the effect of aluminum particle size on propellant burning rate suggests that increased pressure dependence results from smaller aluminum particles and a subsequent transition from diffusionally limited to kinetically limited aluminum particle combustion [13]. In the case of propellants containing Al/PTFE composite particles, the average agglomerate diameter (25 μm) is also similar to the ~10-20 μm size range over which aluminum particles burning in oxygen transition from diffusive to kinetically limited combustion [3]. In general, these results show that modification via fluorocarbon inclusion is highly efficient at reducing aluminum particle size during combustion and can result in kinetically controlled aluminum combustion, but from much larger (~42 μm average diameter) aluminum particles.

Higher magnification examination of collected products from the propellant with Al/PTFE composite particles (Figure 7) indicates the presence of both a coarse (25 μm average particle size) and a fine, sub-micrometer fraction. Electron dispersive spectroscopy of these products indicates the coarse fraction is made up of aluminum and oxygen, while the fine fraction consists of aluminum, oxygen, and fluorine. The atomic ratios of aluminum to oxygen suggest that the coarse fraction is completely oxidized.

The absence of crystalline aluminum in condensed products in the modified propellant is confirmed by X-ray diffraction (Figure 8). Additionally, the presence of aluminum fluoride in Al/PTFE propellant products is also verified. Conversely, baseline spherical aluminized propellant products contain a significant amount of unreacted, crystalline aluminum as well as traces of unreacted ammonium perchlorate. Both propellant products also contain a mixture of a number of different aluminum oxide phases.

4. Conclusions

In summary, this work shows that use of inclusion modified, fuel rich Al/PTFE MA composite particles can result in drastic alteration of the burning characteristics of solid propellants and condensed phase products. During propellant combustion these modified Al particles react from within, rupturing into much smaller aluminum particles that increase the influence of combustion kinetics and result in greater burning rate pressure sensitivity. These overall smaller, faster burning particles ignite promptly at the burning surface, result in improved heat transfer, and more complete aluminum combustion. Finally, these particles result in agglomerate sizes that are smaller than the initial particle size. In comparison to similarly sized spherical aluminum, Al/PTFE inclusion modified particles result in a 66% reduction in agglomerate diameter (a 96% decrease in agglomerate volume), which should translate to a significant decrease in solid rocket propellant two-phase flow loss. Future efforts are focused on producing spherical composite particles and studying

the ignition of single particles at high heating rates comparable to those experienced during propellant combustion.

5. Acknowledgements

The authors would like to acknowledge the financial support of the Air Force Office of Scientific Research under the supervision of Dr. Mitat Birkan (#4792-PU-AFOSR-0004).

6. References

- [1] G. P. Sutton and O. Biblarz, *Rocket Propulsion Elements*, 7th ed. Wiley, 2001.
- [2] K. Jayaraman, S. R. Chakravarthy, and R. Sarathi, "Quench collection of nano-aluminium agglomerates from combustion of sandwiches and propellants," *Proceedings of the Combustion Institute*, vol. 33, pp. 1941–1947, 2011.
- [3] R. A. Yetter, G. A. Risha, and S. F. Son, "Metal particle combustion and nanotechnology," *Proceedings of the Combustion Institute*, vol. 32, no. 2, pp. 1819–1838, 2009.
- [4] D. T. Bui, A. I. Atwood, and T. M. Antienza-More, "Effect of aluminum particle size on combustion behavior of aluminized propellants in PCP binder," presented at the 35th International Annual Conference of ICT, Karlsruhe, 2004.
- [5] O. Orlandi, J.-F. Guery, G. Lacroix, S. Chevalier, and N. Desgardin, "HTPB/AP/AL Solid Propellants with Nanometric Aluminum," presented at the 2005 European Conference for Aerospace Sciences (EUCASS), Moscow, 2005, pp. 1–7.
- [6] Y. Aly, M. Schoenitz, and E. L. Dreizin, "Aluminum-metal reactive composites," *Combustion Science and Technology*, vol. 183, pp. 1107–1132, 2011.
- [7] S. Zhang, C. Badiola, M. Schoenitz, and E. L. Dreizin, "Oxidation, ignition, and combustion of Al-I₂ composite powders," *Combust. Flame*, vol. 159, pp. 1980–1986, 2012.
- [8] S. Zhang, M. Schoenitz, and E. L. Dreizin, "Metastable aluminum-based reactive composite materials prepared by cryomilling," presented at the 50th AIAA Aerospace Sciences Meeting, Nashville, TN, 2012, pp. 1–12.
- [9] L. E. Fried, W. M. Howard, Souers, P. C., and P. A. Vitello, "Cheetah 6.0 User Manual," Lawrence Livermore National Laboratory, Livermore, CA, LLNL-SM-416166, 2010.
- [10] T. R. Sippel, S. F. Son, and L. J. Groven, "Altering reactivity of aluminum with selective inclusion of polytetrafluoroethylene through mechanical activation," *Propellants, Explosives, and Pyrotechnics: in press*, 2012.
- [11] M. C. Hinkelman, "Development and testing of dicyclopentadiene based solid composite propellants," Purdue University, 2011.
- [12] R. Jeenu, K. Pinumalla, and D. Deepak, "Size distribution of particles in combustion products of aluminized composite propellant," *J Propul Power*, vol. 26, no. 4, pp. 715–723, 2010.
- [13] C. R. Zaseck, S. F. Son, and T. L. Pourpoint, "Combustion of micron-aluminum and hydrogen peroxide propellants," *Combust Flame*, vol. 160, pp. 184–190, 2012.

7. Figures

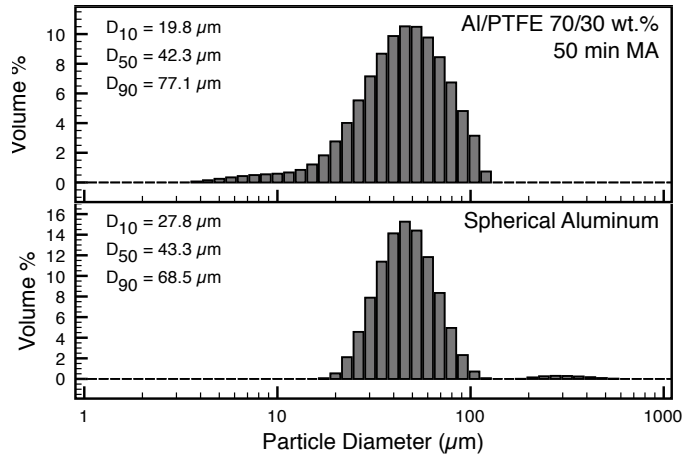


Figure 1 - Particle size distributions of 25-75 μm sieved MA particles and spherical aluminum.

Table 1 - Propellant formulation details, uncured viscosity, and cured density.

Propellant Designation	Propellant Formulation [†]		Uncured Viscosity (30-35°C) (cP)	Cured Density (g/cm ³)	Cured Density (%TMD)
	Metal Type	Metal (wt.%)			
Spherical	Spherical Al	15%	$4.8 \cdot 10^6$	1.68	87.6%
70/30	Al/PTFE 70/30 wt.%, 50 min MA	15%	$4.2 \cdot 10^7$	1.72	90.6%

[†]All propellants contained 71 wt.% AP (80 wt.% 200 μm coarse, 20 wt.% 20 μm fine), 14.0 wt.% HTPB binder, and 15 wt.% aluminum or MA composite (25-75 μm).

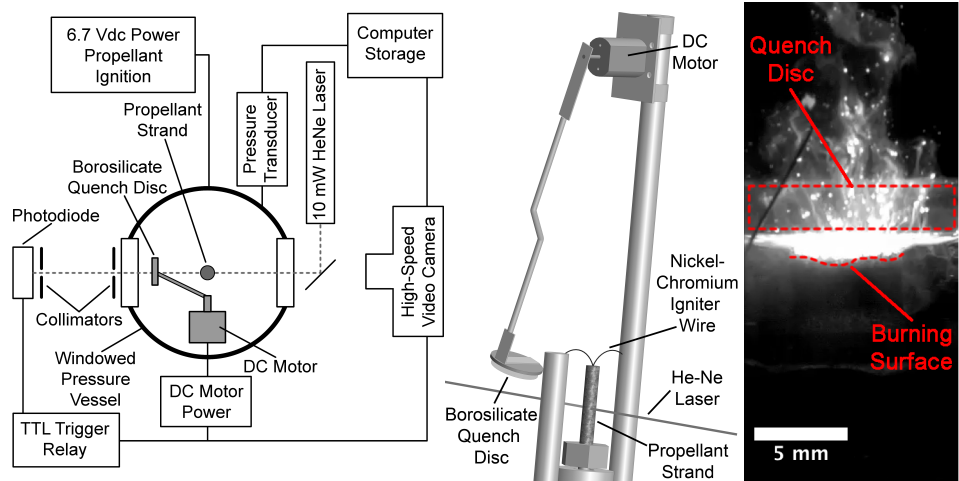


Figure 2 - Diagram of propellant combustion experiment (left), detail showing agglomerate quench device (center), and still frame showing actuation and agglomerate capture (right).

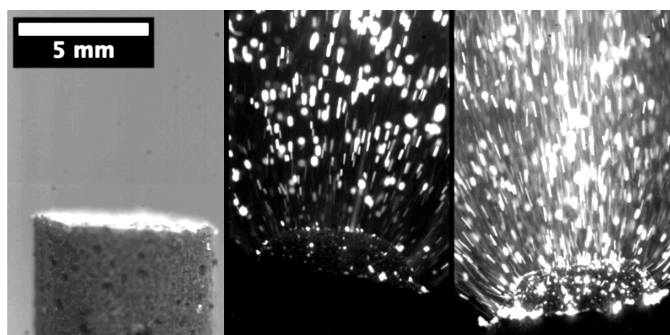


Figure 3 - Solid propellant strand (left) and still images of spherical aluminum (center) and Al/PTFE 70/30 wt.% MA particle (right) containing propellant surfaces burning at 0.1 MPa (14.7 psi). Photos were taken with the same exposure settings.

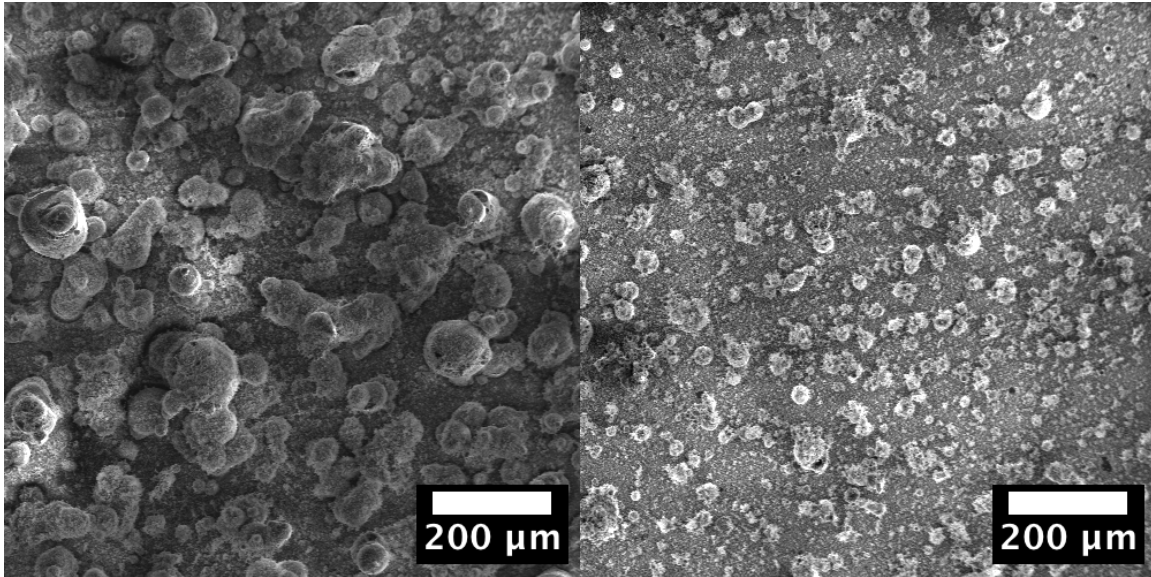


Figure 4 - Scanning electron images of quenched agglomerate products from 6.89 MPa (1000 psi) combustion of propellant containing 25-75 μm spherical aluminum (left) and 25-75 μm Al/PTFE 70/30 wt.% composite particles (right).

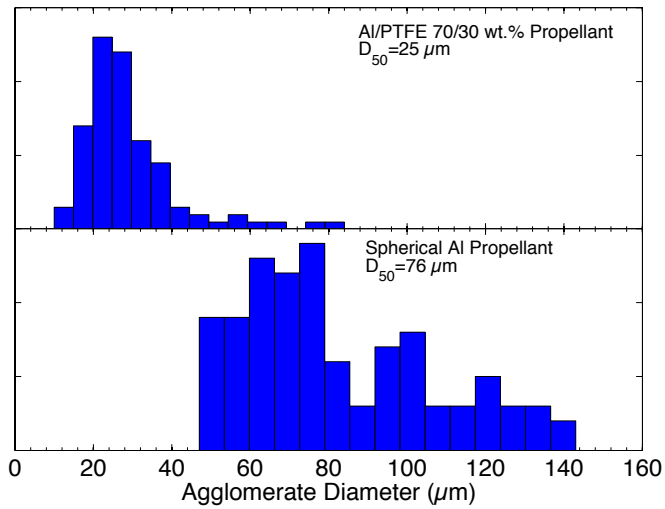


Figure 5 - Size distribution of agglomerated products from propellant combustion (6.89 MPa). Sample size, n=100 for each distribution.

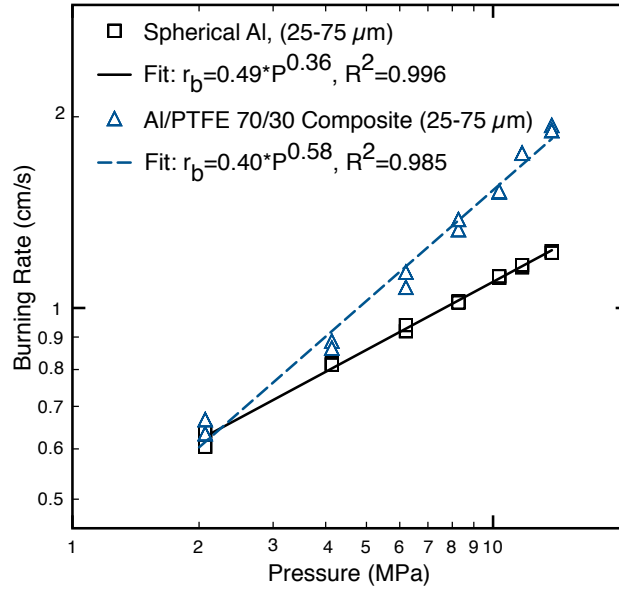


Figure 6 - Solid propellant linear burning rates and power law pressure dependence.

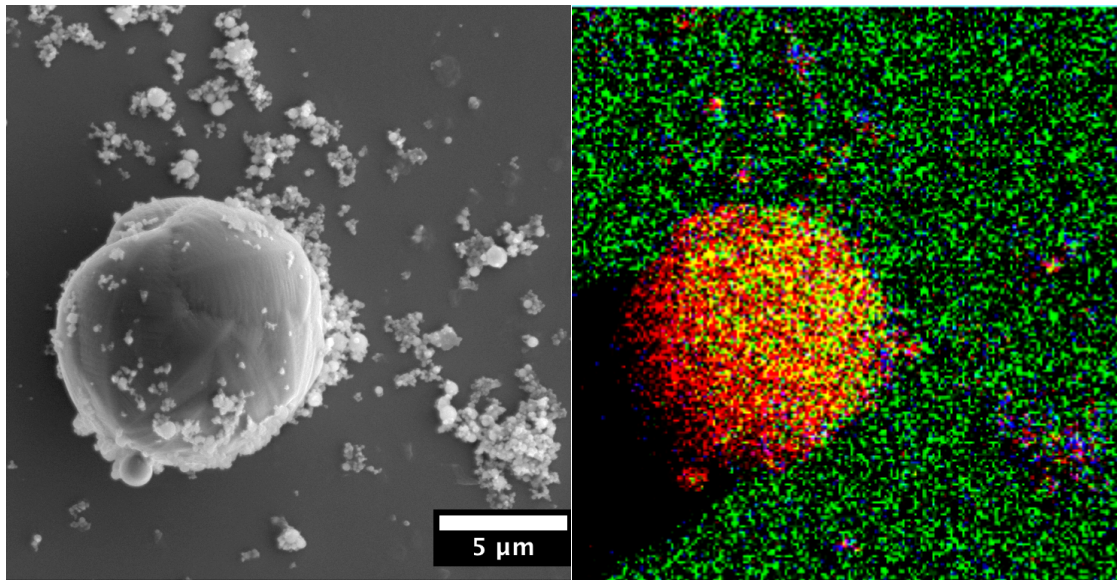


Figure 7 - Electron micrograph (left) and EDS chemical map (right) of quenched products from Al/PTFE 70/30 wt.% MA particle-containing propellant burned at 6.89 MPa (1000 psi). In EDS map, Al = red, oxygen = green, fluorine = blue.

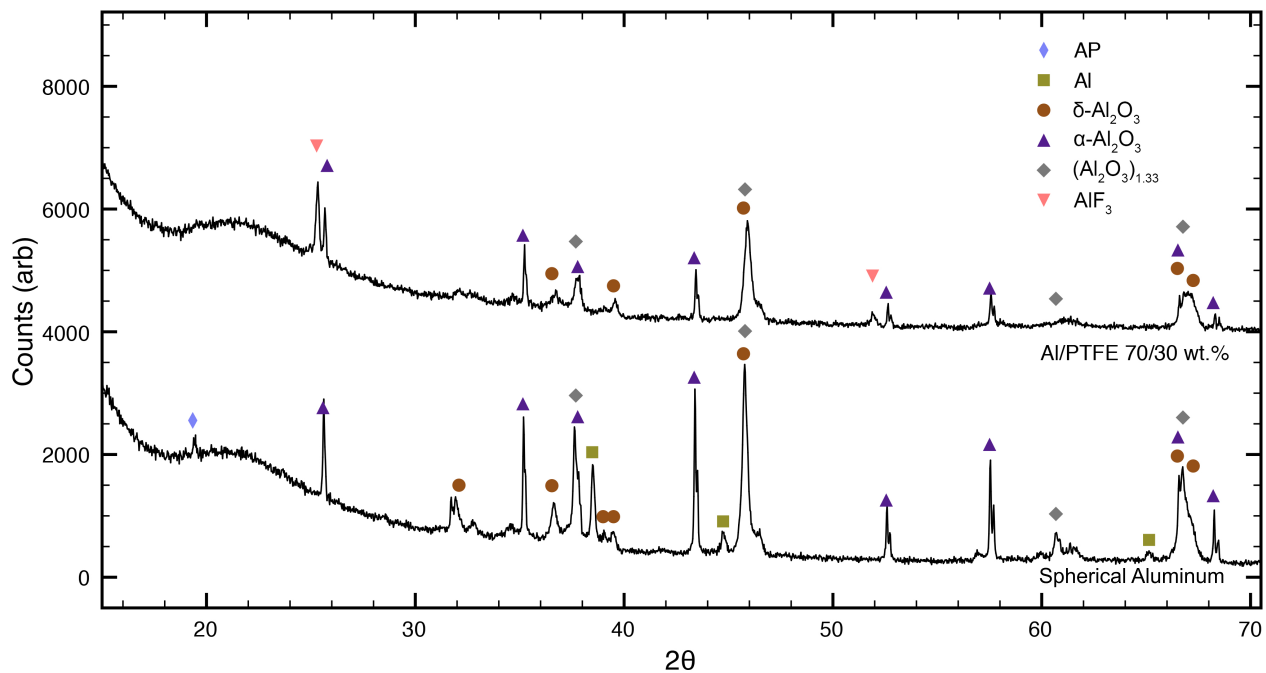


Figure 8 - X-ray diffraction phase composition of products quenched during combustion (6.89 MPa) of propellant containing spherical Al particles (bottom) and Al/PTFE 70/30 wt.% MA particles (top).